

# On the accuracy of GAIA radial velocities

U. Munari, P. Agnolin and L. Tomasella<sup>1</sup>

Osservatorio Astronomico di Padova, Sede di Asiago, I-36012 Asiago (VI), Italy

## Abstract.

We have obtained 782 real spectra and used them as inputs for 6700 automatic cross-correlation runs to investigate GAIA potential in terms of radial velocity accuracy. We have explored the dispersions 0.25, 0.5, 1 and 2 Å/pix over the 8490–8740 Å GAIA range. We have investigated late-F to early-M stars (constituting the vast majority of GAIA targets), slowly rotating ( $\langle V_{rot} \sin i \rangle = 4 \text{ km sec}^{-1}$ ), of solar metallicity ( $\langle [\text{Fe}/\text{H}] \rangle = -0.07$ ) and not binary. The results are accurately described by the simple law:  $\lg \sigma = 0.6 \times (\lg \frac{S}{N})^2 - 2.4 \times \lg \frac{S}{N} + 1.75 \times \lg D + 3$ , where  $\sigma$  is the cross-correlation standard error (in  $\text{km sec}^{-1}$ ) and  $D$  is the spectral dispersion (in Å/pix). The spectral dispersion has turned out to be the dominant factor, with  $S/N$  being less important and the spectral mis-match being a weak player at the lowest  $S/N$ . Our results show that mission-averaged radial velocities of faint GAIA targets ( $V \sim 15 \text{ mag}$ ) can match the  $\sim 0.5 \text{ km sec}^{-1}$  accuracy of tangential motions, provided the observations are performed at a dispersion not less than 0.5 Å/pix.

## 1 Introduction

GAIA is the coming ESA Cornerstone 6 mission. It is designed to obtain extremely precise astrometry (in the micro-arcsec regime), multi-band photometry and medium/high resolution spectroscopy for a large sample of stars. The goals as depicted in the mission *Concept and Technology Study Report* (ESA SP-2000-4, hereafter *CTSR*) call for astrometry and broad band photometry to be collected for all stars down to  $V \sim 20 \text{ mag}$  over the entire sky ( $\sim 10^9$  stars), with brighter magnitude limits for spectroscopy and intermediate band photometry. Each target star should be measured about a hundred times during the five year mission life-time, in a fashion similar to the highly successful *Hipparcos* operation mode. The astrophysical guidelines of the GAIA mission are discussed by Gilmore et al. (1998, 2000) and Perryman et al. (2001), an overview of the GAIA payload and spacecraft is presented by Mérat et al. (1999), while the goals of the GAIA spectroscopy are discussed by Munari (1999, 2001).

The principal aim of GAIA spectroscopy will be to provide the 6<sup>th</sup> component of the phase-space, the radial velocity. The obvious goal of GAIA radial velocities is to parallel the precision of tangential motions. The latter is a combination of the precision of parallaxes and proper motions. From stellar population models of the Galaxy, *CTSR* estimates an average accuracy of  $0.5 \text{ km sec}^{-1}$  for the tangential motions of  $V \sim 15 \text{ mag}$  stars. The latter is close to the magnitude limit of GAIA spectroscopy, the exact one depending on the final optical design, on-board data processing strategies, detection threshold, telemetry constraints and so forth. To appropriately complement the keen astrometric vision of the Galaxy, GAIA radial velocities therefore need to be accurate at their faint magnitude limit.

---

<sup>1</sup>send off-print requests to U.Munari, [munari@pd.astro.it](mailto:munari@pd.astro.it)

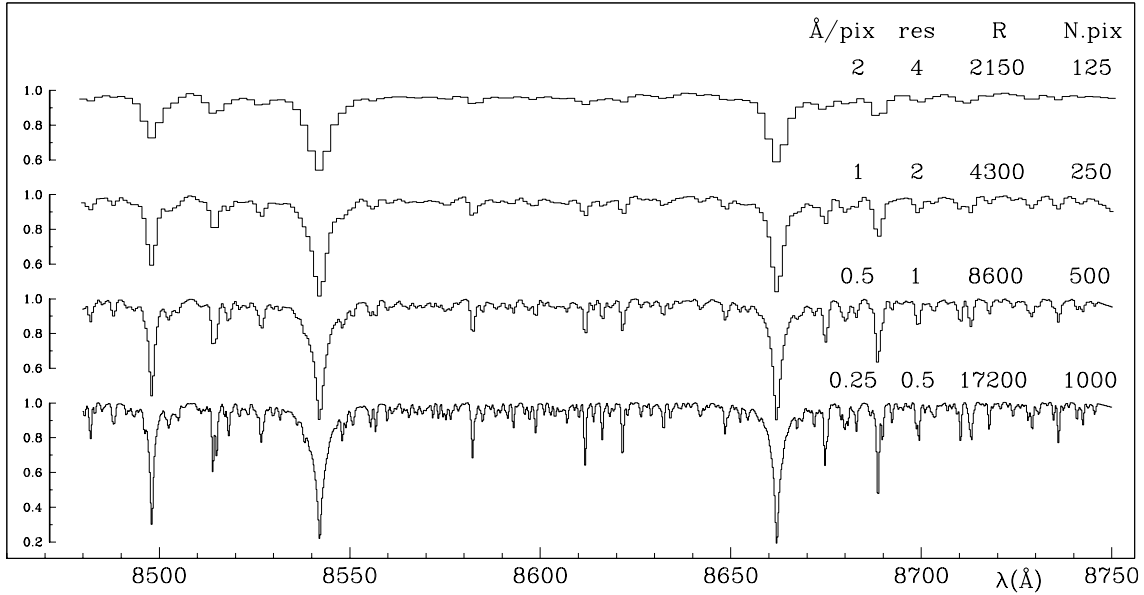


Figure 1: The figure illustrates the effect of degrading the dispersion of GAIA spectra (from one spectrum to the next the dispersion changes by a factor of 2). The  $0.75 \text{ \AA/pix}$  currently baselined for GAIA falls at the center of the explored  $8\times$  range. To focus upon the features carrying RV informations and to avoid disturbance by the necessarily limited S/N of real spectra, synthetic spectra from Munari and Castelli (2000) have been used to produce this figure. The spectra refer to a K0 III star with  $T=4750 \text{ K}$ ,  $\log g=3.0$ ,  $[\text{Z}/\text{Z}_\odot]=0.0$  and  $V_{\text{rot}} \sin i = 5 \text{ km sec}^{-1}$ , i.e. the average program star in Table 1. Over each spectrum the dispersion (in  $\text{\AA/pix}$ ), the resolution (in  $\text{\AA}$ ), the resolving power  $R$  and the spectrum length (in pixels) are given.

GAIA will record spectra covering the  $8490\text{--}8740 \text{ \AA}$  region (cf. Munari 1999), at  $0.75 \text{ \AA/pix}$  dispersion as currently baselined in the CTSR. A  $\Delta\lambda \sim 250 \text{ \AA}$  range is mainly imposed by optical constraints on the maximum  $\lambda$ –interval well focusable over the large field ( $2^\circ \times 1^\circ$ ) of the GAIA spectroscopic focal plane, where CCDs operated in TDI mode will record the spectra as they transit over the field. The GAIA  $8490\text{--}8740 \text{ \AA}$  interval is dominated by the Ca II triplet, which is among the strongest spectral lines at any optical wavelength in F-G-K-M stars. The latter will be the dominating types among GAIA spectroscopic targets (from Galaxy models and Hipparcos/Tycho data, the average color of field stars at  $V = 10$  mag corresponds to a G0 spectral type, and to K0 at  $V = 15$  mag).

The aim of the present paper is to evaluate the *potential* precision of GAIA radial velocities as function of spectral resolution and signal-to-noise ratio. How much of this *potential* precision will be effectively exploited by GAIA will depend upon the control over the wavelength scale of the recorded spectra, which is open to refinements (the *modus operandi* of GAIA spectroscopy being similar to an “objective-grism” approach, where for obvious reasons calibration lamps and/or telluric absorptions cannot be used as in classical ground-based spectra). In this paper we use real data (obtained with real CCDs at real spectrographs+telescopes) and automatic cross-correlation measurement of radial velocities in the attempt to better account – compared to simulations – for all sources of noise, manifest as well as hidden, affecting GAIA observations and data reduction.

This study follows and confirms preliminary investigations we performed and circulated in 1997–98 as internal documents of the ESA Photometric and Spectroscopic Working Group for GAIA (UM-PWG-005, UM-PWG-006).

## 2 Data

### 2.1 Selection of program stars

The late-F to early-M program stars have been selected – according to visibility at the time of the observing runs – among IAU standard RV stars (as listed in the Astronomical Almanac). Three additional bright stars (with no record of binarity, radial velocity variability or spectral peculiarities) were selected to complement the observations at  $0.25 \text{ \AA/pix}$ .

The program stars are listed in Table 1, together with their RVs (from Astronomical Almanac, 2002 edition), rotational velocity (from Glebocki et al. 2000) and metallicity (from Cayrel de Strobel et al. 1997). Their median rotational velocity is  $V_{\text{rot}} \sin i = 4 \text{ km sec}^{-1}$ , which is close to the median value of field stars as shown in Table 2.

### 2.2 Explored dispersions and resolutions

We have explored four dispersions:  $0.25$ ,  $0.5$ ,  $1$  and  $2 \text{ \AA/pix}$ . They bracket the  $0.75 \text{ \AA/pix}$  currently baselined for GAIA.

Figure 1 is a visualization of these dispersions upon the same K0 III synthetic spectrum (with  $V_{\text{rot}} \sin i = 4 \text{ km sec}^{-1}$  and  $[\text{Z}/\text{Z}_{\odot}] = 0.0$ , from Munari and Castelli 2000). Throughout this paper the spectral resolution (taken as the FWHM of the PSF) is kept constant at 2.0 pixels. Therefore the resolutions explored in this paper are  $0.5$ ,  $1$ ,  $2$  and  $4 \text{ \AA}$  corresponding to resolving powers  $R=17\,200$ ,  $8\,600$ ,  $4\,300$  and  $2\,150$ .

### 2.3 Strategy

The mean uncertainty upon the RVs of the IAU standard stars in Table 1 is  $0.23 \text{ km sec}^{-1}$  which corresponds to a mean uncertainty of  $0.33 \text{ km sec}^{-1}$  in the RV difference between two program stars. This is comparable to the expected error of the cross-correlation at the highest dispersion and S/N here investigated. For this and other reasons, to estimate the error of the cross-correlation we decided to proceed in a way independent from the exact knowledge of the individual RVs. It only requires the RV constancy of the given program star during the 0.5–1.5 hours of observation, which is certainly the case for IAU standard RV stars.

For each dispersion and program star we obtained three deep spectra that were combined into a single high S/N template ( $\text{S/N} \geq 220$ ). We then proceeded for each program star to obtain five spectra at  $\text{S/N} \sim 110$ , five spectra at  $\text{S/N} \sim 35$  and other five spectra at  $\text{S/N} \sim 10$  by properly adjusting the exposure time. The final extracted spectra had an average S/N per pixel of the continuum of  $110$ ,  $33$  and  $12$ , respectively.

For each program star we then cross-correlated the five spectra at  $\text{S/N} \sim 110$  against the high S/N template and derived a standard deviation of the resulting radial velocities. The same was done for the five  $\text{S/N} \sim 33$  spectra and for the five at  $\text{S/N} \sim 12$ . To increase the statistics and to account for possibly large mis-matches between objects and templates in the GAIA automatic cross-correlations, the  $5+5+5$  object spectra of each

		RV (km sec <sup>-1</sup> )	V <sub>rot</sub> sin i (km sec <sup>-1</sup> )	[Fe/H]	Disp. (Å/pix)			
					0.25	0.5	1	2
HD 222368	F7 V	+5.3 ± 0.2	6.5 ± 0.6	-0.27 ± 0.06	X			
HD 187691	F8 V	+0.1 ± 0.3	3.7 ± 0.5	+0.12 ± 0.01		X	X	
HD 136202	F8 IV-V	+53.5 ± 0.2	4.7 ± 0.1	-0.13 ± 0.04	X	X	X	
HD 102870	F9 V	+5.0 ± 0.2	5.9 ± 0.9	+0.20 ± 0.02	X	X		
HD 154417	G0 V	-17.4 ± 0.3	5.5 ± 0.4	-0.18 ± 0.01	X	X	X	
HD 126053	G1 V	-18.5 ± 0.4	2.4 ± 1.0		X	X	X	
HD 145001	G5 III	-9.5 ± 0.2	9.9 ± 0.1	-0.26	X	X		
HD 21120	G6 III		5.5 ± 0.3		X			
HD 182572	G7 IV	-100.5 ± 0.4	2.0 ± 0.2	+0.38 ± 0.04		X		
HD 144579	G8 V	-60.0 ± 0.3				X	X	
HD 103095	G8 V	-99.1 ± 0.3	3.0 ± 1.1	-1.35 ± 0.04			X	
HD 194071	G8 III	-9.8 ± 0.1				X		
HD 48329	G8 I		8.5 ± 0.6	-0.06 ± 0.01	X			
HD 3712	K0 III	-3.9 ± 0.1	5.0 ± 0.1	-0.10 ± 0.04	X			
HD 107328	K0 III	+35.7 ± 0.3	2.7 ± 1.0	-0.38 ± 0.12		X	X	
HD 212943	K0 IV-III	+54.3 ± 0.3	1.0 ± 0.5	-0.33 ± 0.03		X	X	
HD 132737	K1 III	-24.1 ± 0.3				X	X	
HD 12929	K2 III	-14.3 ± 0.2	1.8 ± 0.6	-0.22 ± 0.03	X			
HD 161096	K2 III	-12.0 ± 0.1	2.4 ± 0.6	+0.05 ± 0.04	X		X	
HD 186791	K3 II	-2.1 ± 0.2	3.5 ± 0.3	-0.15 ± 0.08	X	X		
HD 213947	K4 III	+16.7 ± 0.3					X	
HD 29139	K5 III		2.8 ± 0.4	-0.09 ± 0.06	X			
HD 146051	M0 III	-19.8 ± 0.0		+0.32		X	X	X
HD 18884	M2 III	-25.8 ± 0.1			X			

Table 1: Program stars. The radial velocities are from *Astronomical Almanac 2002*, rotational velocities from Glebocki et al. (2000) and metallicities from Cayrel de Strobel et al. (1997). The last four columns indicate the dispersions at which the program stars have been observed.

	F0	F5	G0	G5	K0	K5	M0
V	83	18	5	6	6	6	4
III	73	50	14	6	5	2	3

Table 2: Median V<sub>rot</sub> sin i (in km sec<sup>-1</sup>) are computed for selected spectral classes from the data in the Glebocki et al. (2000) catalogue of rotational velocities for about 12 000 field stars. Stars of luminosity class I stars are generally undersampled in the catalogue and thus not considered in this table.

cross-corr. error (km sec <sup>-1</sup> )			cross-corr. error (km sec <sup>-1</sup> )						
S/N=110 S/N=33 S/N=12			S/N=110 S/N=33 S/N=12						
0.25 Å/pix			0.5 Å/pix						
HD 222368	F7 V	0.26	0.59	1.59	HD 136202	F8 III	0.94	1.43	2.22
HD 21120	G6 III	0.60	0.80	0.60	HD 102870	F9 V	0.96	1.44	4.70
HD 48329	G8 I	0.29	0.29	1.05	HD 154417	G0 V	1.10	1.52	4.01
HD 3712	K0 III	0.08	0.15	0.77	HD 126053	G1 V	1.09	1.82	4.02
HD 12929	K2 III	0.28	0.38	1.09	HD 182572	G7 IV	2.17	1.91	4.27
HD 29139	K5 III	0.55	0.87	1.62	HD 145001	G8 III	1.37	1.84	3.55
HD 18884	M2 III	0.51	0.75	1.26	HD 161096	K2 III	1.16	1.43	1.92
					HD 186791	K3 II	1.02	1.72	1.91
					HD 146051	M0 III	0.60	1.27	1.51
1 Å/pix			2 Å/pix						
HD 187691	F8 V	3.7	3.6	10.4	HD 187691	F8 V	12.0	11.2	21.8
HD 136202	F8 III	3.8	4.0	7.1	HD 103095	F8 III	5.1	22.1	35.8
HD 101870	F9 V	4.9	8.5	13.2	HD 154417	G0 V	10.3	7.9	69.6
HD 154417	G0 V	2.0	2.4	13.1	HD 126053	G1 V	8.2	13.5	17.5
HD 126053	G1 V	3.9	3.5	13.9	HD 103095	G8 V	34.8	49.7	82.5
HD 144579	G8 V	5.0	7.9	8.5	HD 144579	G8 V	22.4	32.4	74.6
HD 145001	G8 III	4.6	5.5	9.9	HD 107328	K0 III	9.2	14.1	23.6
HD 194071	G8 III	2.8	5.0	13.8	HD 132737	K0 III	13.0	9.8	54.3
HD 107328	K0 III	9.0	9.7	15.1	HD 212943	K0 IV-III	13.1	12.3	34.5
HD 132737	K0 III	5.5	6.0	10.3	HD 161096	K2 III	10.6	10.3	13.9
HD 212943	K0 IV-III	6.4	8.8	11.6	HD 146051	M0 III	18.1	15.8	12.9
HD 186791	K3 II	5.5	5.9	10.4					
HD 213947	K4 III	3.5	4.2	6.7					
HD 146051	M0 III	1.8	3.6	6.3					

Table 3: Errors of radial velocities obtained via cross-correlation (in km sec<sup>-1</sup>). The values reported are the mean of the standard deviations of the cross-correlation results when the spectra of the given program star are cross-correlated against the templates of *all* program stars at the given dispersion.

given star were cross-correlated against the *template* spectra of all program stars (at the given dispersion) and the average standard deviation is given in Table 3.

## 2.4 Observations

The observations have been obtained during four nights in 2000 (Jun 15, 21 and 22) and 2001 (Jan 14). The spectra at a given dispersion have been all secured during the same night under identical and very stable instrumental conditions. On a few more nights the observing program could not be completed because of intervening clouds, and data obtained under such circumstances have not been further used in this paper. To complete the observations on a given star at a given dispersion, about one hour was generally enough.

The 0.25 and 0.5 Å/pix pointed observations have been obtained with the Echelle+CCD spectrograph attached to the 1.82 m telescope operated in Asiago by Osservatorio Astronomico di Padova (Italy). An OG455 filter was used to eliminate the cross-disperser second order. The 8490-8740 Å range is covered by 1000 pixels (500 for the 0.5 Å/pix dispersion) and it is fully contained within one Echelle order. For both dispersions the spectrograph slit width was adjusted so that FWHM(PSF) = 2.0 pixels.

The 1 and 2 Å/pix pointed observations were secured with the B&C+CCD spectrograph attached to the 1.22 m telescope operated at Asiago by the Dept. of Astronomy of the University of Padova (Italy). A 1200 and a 600 ln/mm gratings were used together with an RG1 filter to eliminate the grating second order. Again, for both dispersions the spectrograph slit width was adjusted so that FWHM(PSF) = 2.0 pixels.

## 2.5 Cross-correlations

The cross-correlations were performed via the `fxcor` task in IRAF, operated in automatic batch mode (plus some custom codes in C++). A total of 6705 cross-correlation runs were performed on the 782 input spectra.

We used pixel-based extracted spectra, without wavelength calibration to avoid to introduce spurious effects and to better simulate the GAIA data. Observations obtained with a Cassegrain telescope suffer from thermal changes and mechanical flexures, which will be absent in GAIA. Accurate cross-correlation of the rich telluric absorption forest (cf. Munari 1999) flanking on both side the GAIA wavelength region has been used to compensate for the the spectrograph's focal plane drift over the CCD. The minimal thermal changes in the dome during the observations produced unnoticeable focal plane drifts, while the mechanical flexures could always been compensated for by cross-correlation between the telluric lines in the *template* and *object* spectra. The mechanical flexures matched their mathematical modeling by Munari and Lattanzi (1992).

## 3 Results

To further filter out the noise due to limited number statistics and to better characterize the role of dispersion and S/N, the star-by-star data of Table 3 are averaged in Table 4. The latter can be simply read as the standard error – at a given dispersion and S/N – of the cross-correlation between an object and a template randomly chosen among late-F/early-M spectral types at any luminosity class (with average  $V_{\text{rot}} \sin i = 4 \text{ km sec}^{-1}$  and  $[Z/Z_{\odot}] = 0.0$ ). Table 5 lists for each dispersion the magnitudes of the stars observed by GAIA that provide spectra of the given S/N per single passage over the field of view.

### 3.1 The role of spectral dispersion and S/N

The data in Table 4 are well fitted by the simple law:

$$\lg \sigma = 0.6 \times (\lg \frac{S}{N})^2 - 2.4 \times \lg \frac{S}{N} + 1.75 \times \lg D + 3 \quad (1)$$

where  $\sigma$  is the standard error in  $\text{km sec}^{-1}$ ,  $\frac{S}{N}$  is obviously the signal-to-noise ratio (per pixel on the stellar continuum) and  $D$  is the spectral dispersion (in Å/pix).

The effect of S/N (at least over the 12 – 110 range here explored) is pretty similar at all investigated dispersions: going from S/N=12 to S/N=33 doubles the accuracy of RVs, while an increase from S/N=33 to S/N=110 increases the precision of RVs by only 35%.

It is therefore clear from Table 4 and Figure 2 that the dispersion is the principal factor governing the potential accuracy of GAIA radial velocities, with S/N playing a less important role: pushing the exposure time so long to achieve S/N~110 does not provide more accurate results than obtainable with S/N~12 spectra at twice better resolution.

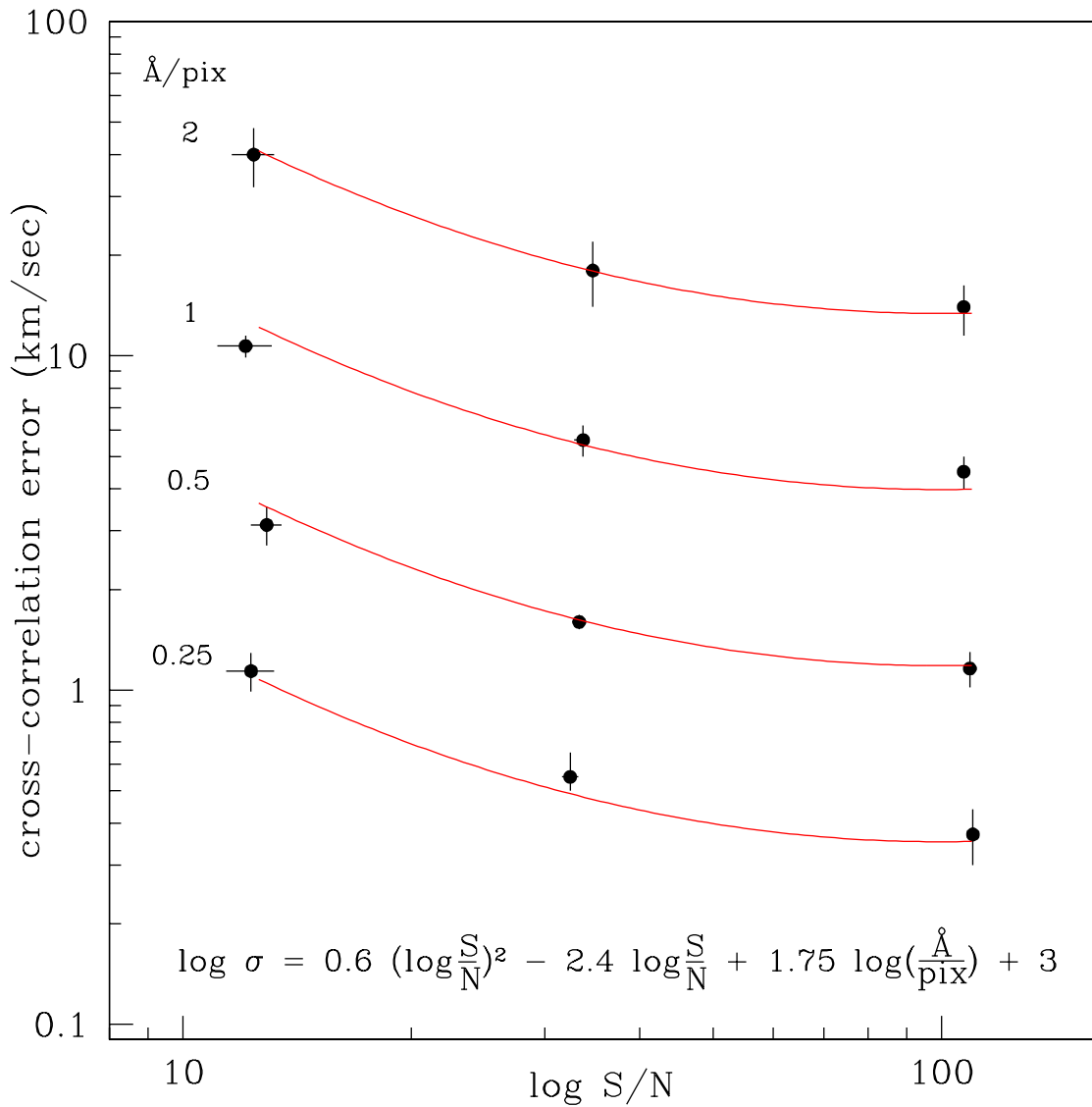


Figure 2: The results of Table 4 in graphical form. The results for each individual dispersion show the same dependence upon S/N. This is emphasized by the fitting curves obtained from the expression for  $\lg \sigma$  by inserting the appropriate value of the dispersion (in  $\text{\AA}/\text{pix}$ ).

Disp. (Å/pix)	[12]		[33]		[110]	
	$\langle S/N \rangle$	$\langle \sigma \rangle$	$\langle S/N \rangle$	$\langle \sigma \rangle$	$\langle S/N \rangle$	$\langle \sigma \rangle$
0.25	12.3±0.9	1.14±0.15	32.4±0.8	0.55±0.10	110±1.7	0.37±0.07
0.5	12.9±0.6	3.12±0.41	33.3±0.7	1.60±0.08	109±1.3	1.16±0.14
1	12.1±1.0	10.7±0.8	33.7±0.5	5.6±0.6	107±1.9	4.5±0.5
2	12.4±0.8	40±8	34.7±0.5	18±4	111±1.6	14±2.5

Table 4: The accuracy of radial velocities obtained via cross-correlation for late-F to early-M stars as function of S/N and spectral dispersion. The reported values are grand-averages over the results of Table 3 and the uncertainties are formal errors of the mean. 12, 33 and 110 refer to the average S/N of each group.

### 3.2 The effect of mis-match

Equation (1) is affected by the mis-match between *template* and *object* spectra. To account for it too would have required an unrealistic observational effort (about  $30\times$  more spectra, in the neighborhood of 25 000 total). Therefore, the systematic exploration of the (minor) role played by mis-match in spectral type, metallicity and rotational velocity can only be performed via cross-correlation of huge databases of *synthetic* spectra (Zwitter 2001, in preparation). A few preliminary considerations are however in order, separately for low and high S/N spectra.

For S/N=12 and S/N=33 spectra, we can roughly and preliminary estimate it only for K0/K1 program stars and for 1 and 2 Å/pix dispersions, for which at least three such stars were observed. A check on the original data (not reported here for their excessive length) show that cross-correlating 1 or 2 Å/pix spectra of K0/1 IV/III program stars with templates of the same spectral types produces  $\sim 15\%$  better results than cross-correlation with templates of largely different spectral types chosen between the late-F/early-M boundaries. Such a result is readily appreciable when the 1 and 2 Å/pix spectra in Figure 1 are considered: at these low dispersions only the three Ca II and a few Fe I lines carry RV information and the same lines are always and invariably the dominating features in the spectra of the late-F to early-M stars (cf. the GAIA spectral atlases of Munari and Tomasella 1999, Munari and Castelli 2000 and Castelli and Munari 2001).

For S/N=110 spectra, the mis-match is expected to be proportionally more important. Whatever high the S/N might be, unavoidable differences remain in *template* and *object* spectra simply because they are intrinsically different and this places a physical limit to the accuracy the cross-correlation can achieve.

In conclusion, in absence of mis-match it could be expected the fitting lines in Figure 2 to be less curved and more straight at the higher S/N, maintaining however the same spacing among them and the same slope at the lower S/N. Put in other words, a proper account for mis-match would have only minor effects at low S/N while it is expected to improve more significantly the accuracy achievable with high S/N data. Therefore, to exploit the best intrinsic accuracy of the highest signal-to-noise GAIA spectra it will be necessary to accurately determine and use the best possible template for each individual spectrum (that will however concern a minimal part of the GAIA spectra for which an *ad hoc* reduction pipeline can be envisaged if necessary).

$\text{\AA}/\text{pix}$	S/N	$I_C$	$V_{\text{F5V}}$	$V_{\text{G5V}}$	$V_{\text{K5V}}$
0.25	110	7.80	8.31	8.52	9.13
	33	10.41	10.92	11.13	11.74
	12	12.61	13.12	13.33	13.94
0.50	110	8.55	9.06	9.27	9.88
	33	11.16	11.67	11.88	12.49
	12	13.36	13.87	14.08	14.69
0.75	110	8.99	9.50	9.71	10.32
	33	11.60	12.11	12.32	12.93
	12	13.80	14.31	14.52	15.13
1.00	110	9.30	9.81	10.02	10.63
	33	11.92	12.43	12.64	13.25
	12	14.11	14.62	14.83	15.44
2.00	110	10.06	10.57	10.78	11.39
	33	12.70	13.21	13.42	14.03
	12	14.87	15.38	15.59	16.20

Table 5: The table provides the magnitudes of the stars observed by GAIA that correspond to the explored S/N (per pixel) at the given dispersion per single passage over the field of view. The magnitudes are computed for the Cousins'  $I$  band, which covers the wavelength range of GAIA spectra. The corresponding  $V$  magnitudes are listed for F5 V ( $V - I_C = +0.51$ ), G5 V ( $V - I_C = +0.72$ ) and K5 V ( $V - I_C = +1.33$ ) unreddened stars. The following parameters have been adopted in the computations: mirror size =  $75 \times 70$  cm; overall throughput = 35%; crossing time = 60.8 sec;  $I_C^{mag=0.0} = 1.196 \times 10^{-9}$  erg  $\text{cm}^{-2} \text{ sec}^{-1} \text{ \AA}^{-1} = 519$  photons  $\text{cm}^{-2} \text{ sec}^{-1} \text{ \AA}^{-1}$ ; R.O.N. =  $3 e^{-1}$ ; dark =  $0.01 e^{-1} \text{ sec}^{-1}$ ; sky background  $I_C = 21.5 \text{ mag arcsec}^{-2}$ .

### 3.3 Instrumental stability

A careful control over the instrumental conditions and stability was maintained during the acquisition of the 782 input spectra used for this paper. As a side test, we obtained a further set of 0.25 Å/pix spectra under non-stable conditions (typically one object per night between June 17 and June 25 2000, with grating and slit moved back and forth and spectrograph refocused during day-time, and with appreciable thermal cycles  $\Delta T \sim 4\text{--}8$  °C from day to night; several colleagues kindly offered a short part of their observing time for the purpose). The data were then extracted and the spectra cross-correlated in exactly the same manner as described for the main data. The result of these additional 0.25 Å/pix observations, aimed to simulate poor environmental and instrumental control over GAIA observations, are:  $\langle \sigma \rangle = 2.95 \text{ km sec}^{-1}$  at  $\langle S/N \rangle = 14$ ,  $\langle \sigma \rangle = 1.53 \text{ km sec}^{-1}$  at  $\langle S/N \rangle = 35$  and  $\langle \sigma \rangle = 1.03 \text{ km sec}^{-1}$  at  $\langle S/N \rangle = 106$ . They are only marginally better than the values reported in Table 4 for the 0.5 Å/pix dispersion. A poor thermal/mechanical stability has therefore vanished the gain expected from a twice higher dispersion. This (obvious) result stresses the advantages of the unique and very favorable GAIA environment, characterized by extreme mechanical and thermal stability.

## 4 Discussion

Our investigation has shown that mission-averaged radial velocities of faint GAIA targets ( $V \sim 15$  mag) can match the  $\sim 0.5 \text{ km sec}^{-1}$  accuracy of tangential motions, provided the observations are performed at a dispersion not less than 0.5 Å/pix. From Table 4 and Figure 2 a  $S/N=10$  spectrum at 0.5 Å/pix dispersion has a standard error of  $\sim 5 \text{ km sec}^{-1}$ , and a hundred such spectra are necessary to lower the error on the mean velocity to 0.5  $\text{km sec}^{-1}$ . This is valid for *single* stars of the dominating GAIA target population, i.e. slow rotating late-F to early-M stars. Binary and/or hotter and/or faster rotating and/or pulsating stars will require a higher accuracy for individual radial velocities (and thus presumably a higher dispersion) to match the  $\sim 0.5 \text{ km sec}^{-1}$  precision of GAIA tangential motions at  $V \sim 15$  mag.

The results of the present observational study agrees with the findings of numerical simulations cited in the CTSR that call for mission-averaged RVs of faint GAIA cool targets to be accurate to  $\sim 5 \text{ km sec}^{-1}$ . This agrees with the results in Table 4 and Figure 2 for the 0.75 Å/pix dispersion baselined for GAIA when proper allowance is made for possible binary nature and/or pulsational activity of the target stars.

The way GAIA will control the zero-point of the wavelength scale of its spectra reinforces the quest for a high spectral dispersion. The determination of the zero-point will be provided by (a) centering of the zero-order image on the spectrograph focal plane, and/or (b) accurate knowledge of the focal plane geometry (as mapped by standard RV stars observed during the mission) + astrometric position of the target stars. The accuracy of both methods can be expressed as a centering error in pixels, and it is obvious that the higher the spectral dispersion the less km sec $^{-1}$  correspond to a 1-pixel shift.

We have shown how the spectral dispersion is the key factor in governing the accuracy of radial velocities. To increase the S/N per pixel on the stellar continuum from  $S/N \sim 12$  to  $S/N \sim 110$  requires  $\sim 80 \times$  more photons. However, a  $S/N \sim 110$  spectrum cannot provide a radial velocity significantly more accurate than a  $S/N \sim 12$  spectrum obtained at twice higher resolution, which costs only  $2 \times$  more photons.

It is also worth to remind that the higher the dispersion, the wider the usage and

interest of the spectra. Spectra of high enough dispersion allow – for instance – rotational velocities and chemical abundances to be measured with confidence. Lowering the dispersion in favor of a higher S/N per pixel (GAIA exposure time is the same for all stars and set by the spacecraft axial rotation period and angular extent of the imaged field of view) does not seem a viable alternative. In fact, when the rotation broadening become sub-pixel it cannot be reliably measured (15 km sec<sup>-1</sup> corresponds to 0.43 Å at GAIA wavelengths, and the majority of GAIA targets will be rotating slower than 15 km sec<sup>-1</sup>, cf. Table 2). Similarly, a low dispersion means severe line blending and the impossibility of element-by-element chemical analysis. On the other hand the higher the dispersion, the more complicate the spectrograph realization and heavier the demands on down-to-Earth telemetry budget. It is easy to anticipate that a lot of work will still be necessary during the final design phase for GAIA to find the best compromise between science demands and technical challenges.

Hot stars (O, B and A types) have not been considered in this paper because they will account for a small fraction of GAIA targets. Preliminary results that we have circulated in 1997 and 1998 among the ESA Photometric and Spectroscopic Working Group for GAIA show that the accuracy of radial velocity rapidly degrades moving toward hotter spectral types (Paschen lines are a weaker spectral feature than Ca II triplet lines). These preliminary results need however refinements and to this aim we have already started the acquisition at the telescope of a large sample of suitable spectra of O, B and A stars to be used in a coming investigation paralleling the present one. Finer analysis of the role of rotation, spectral mis-match and metallicity (the higher the metallicity, the stronger the absorption lines and therefore the stronger the radial velocity signature in the cross-correlation) are also in order and will be considered elsewhere (Zwitter 2001, in preparation).

Finally, it is also worth to remind that these results are relevant not only within the GAIA context but also to ground-based observers because the absence of telluric absorptions and proximity to the wavelengths of peak emission make the explored 8490–8740 Å interval an interesting option for studies of cool stars with conventional telescopes.

*Acknowledgements.* We would like to thank R. Barbon, T. Zwitter and T. Tomov for useful discussions and comments on an early draft of the paper.

## References

Castelli F., Munari U. 2001, A&A 366, 1003  
 Cayrel de Strobel G., Soubiran C., Friel E.D., Ralite N., Francois P. 1997,  
 A&AS 124, 299  
 Gilmore G., Perryman M., Lindegren L., Favata F., Hoeg E., Lattanzi M., Luri X.,  
 Mignard F., Roeser S., de Zeeuw P.T., 1998, Proc SPIE Conference 3350, p. 541  
 Gilmore, G. F., de Boer, K. S., Favata, F., Hoeg, E., Lattanzi, M. G.,  
 Lindegren, L., Luri, X., Mignard, F., Perryman, M. A. C., de Zeeuw, P.T. 2000  
 Proc SPIE Conference 4013, p. 453  
 Glebocki R., Gnacinski P., Stawikowski A. 2000, Acta Astron. 50, 509  
 Mérat P., Safa F., Camus J.P., Pace O., Perryman M.A.C. 1999, in Proceedings

of the ESA Leiden Workshop on GAIA, 23-27 Nov 1998, Baltic Astronomy, 8, 1

Munari U. 1999, in Proceedings of the ESA Leiden Workshop  
on GAIA, 23-27 Nov 1998, Baltic Astronomy, 8, 73

Munari U., 2001, in Proceedings of the Les Houches School "GAIA: the Galaxy Census"  
ed.s C.Turon, O.Bienayme, in press

Munari U., Castelli F. 2000, A&AS 141, 141

Munari U., Lattanzi M.G. 1992, PASP 104, 121

Munari U., Tomasella L. 1999, A&AS 137, 521

Perryman, M. A. C., de Boer, K. S., Gilmore, G., Hoeg, E., Lattanzi, M. G.,  
Lindegren, L., Luri, X., Mignard, F., Pace, O., de Zeeuw, P. T. 2001, A&A 369, 339